



CFD Simulation of flow through pipe fittings

Internship Report
CFD-FOSSEE Team
Indian Institute of Technology Bombay

Prepared by
Mukund S
BMS College of Engineering, Banglore

Under the supervision of
Prof. Manaswita Bose



INDIAN INSTITUTE OF TECHNOLOGY BOMBAY



ACKNOWLEDGEMENT

The following report was created as a part of FOSSEE semester long internship and I would like to thank FOSSEE, Indian Institute of Technology, Bombay for giving me this opportunity.

I would like to thank my project guide Prof. Manaswita Bose, Mentors Mr. Divyesh Variya and Mr. Ashley Melvin for the support in carrying out simulations through out the internship. I would also like to thank project manager Ms. Swetha Manian for giving me this opportunity.

I would like to extend my gratitude to Head, Department of Energy Science and Engineering, Indian Institute of Technology Bombay for giving the permission to use experimental data for validation and Swapnil Raut for helping with details and support.

Mukund S
BMS College of Engineering, Bangalore
Date: September 1, 2021

Contents

I	Case Study 3: Flow through smooth and sharp bends	1
1	Introduction	2
1.1	Aim	2
1.2	Theory	2
1.2.1	Major Losses	2
1.2.2	Minor Losses	3
1.3	Problem Statement	3
1.4	Schematic Diagram	5
2	OpenFOAM base case	6
2.1	pitzDaily	6
2.1.1	Folder Structure	6
2.2	Solver	7
2.2.1	Turbulence Model	8
3	OpenFOAM Case Modifications	9
3.1	Pre-processing	9
3.2	Boundary conditions	9
3.3	Physical properties	10
3.4	fvSchemes & fvSolution	10
3.5	Control parameters	10
3.6	Post-processing	11
4	Results	12
4.1	Numerical Results	12
4.1.1	Smooth Bend	12
4.1.2	Sharp Bend	15



4.1.3	Minor Loss Factors	19
5	Conclusion	23

List of Figures

1.1	Sharp Bend[1]	4
1.2	Smooth Bend[1]	4
1.3	Schematic layout of pipe network with fittings[1]	5
1.4	Pipe Bend	5
4.1	Contours	13
4.2	Pressure Contour	14
4.3	Velocity Contour	15
4.4	Dean vortices	15
4.5	Dean vortices for Higher Reynolds number	16
4.6	Dean vortices for Lower Reynolds number	16
4.7	Contours	16
4.8	Pressure Contour	17
4.9	Velocity Contour	18
4.10	Dean vortices	19
4.11	Dean vortices for Higher Reynolds number	19
4.12	Dean vortices for Lower Reynolds number	20

List of Tables

2.1	Folder contents	7
3.1	Boundary conditions	10
4.1	Literature Values v/s CFD values	20
4.2	CFD results for smooth bend	21
4.3	CFD results for sharp bend	22

Part I

Case Study 3: Flow through smooth and sharp bends

Chapter 1

Introduction

1.1 Aim

The aim of this case study was to determine the minor loss factor of smooth and sharp bend of pipes through CFD method. OpenFOAM version 1912 was used for carrying out the simulation. Further, the velocity and pressure contours of the flow were studied. The study was performed for a 3-D incompressible flow with water as the working fluid, simpleFoam steady state solver was used and κ - ω SST RANS model was adopted to simulate the turbulent flow. The results were viewed in ParaView 5.7.0

1.2 Theory

The resistance to flow in a pipe network causes loss in the pressure head along the flow. The overall head loss across a pipe network consists of the following:

- Major losses
- Minor losses

1.2.1 Major Losses

Major losses refer to the losses in pressure head of the flow due to friction effects. Such losses can be evaluated by using the Darcy-Weisbach equation:

$$h_{major} = f \frac{Lv^2}{2gD} \quad (1.1)$$



where f is the Darcy friction factor, L is the length of the pipe segment, v is the flow velocity, D is the diameter of the pipe segment, and g is acceleration due to gravity. Equation 1.1 is valid for any fully developed, steady and incompressible flow. The friction factor f can be calculated by the following empirical formula, known as the Blasius formula, valid for turbulent flow in smooth pipes with $Re_D < 10^5$:

$$f = 0.316Re_D^{-0.25} \quad (1.2)$$

1.2.2 Minor Losses

In a pipe network, the presence of pipe fittings such as bends, elbows, valves, sudden expansion or contraction causes localized loss in pressure head. Such losses are termed as minor losses. Minor losses are expressed using the following equation:

$$h_{minor} = K \frac{v^2}{2g} \quad (1.3)$$

where K is called the Loss Coefficient of the pipe fitting under consideration. Minor losses are also expressed in terms of the equivalent length of a straight pipe (L_{eq}) that would cause the same head loss as the fitting under consideration:

$$h_{minor} = K \frac{v^2}{2g} = f \frac{L_{eq} v^2}{2gD} \quad (1.4)$$

$$L_{eq} = K \frac{D}{f} \quad (1.5)$$

In the present study, we shall determine the head losses across smooth and sharp bend. Loss of head due to bend in pipe: This is the energy loss due to bend. When a bend is provided in the pipeline, there is a change in direction of the velocity of flow Figure 1.1 and 1.2. Due to this, the flow separates from the walls of the bend and formation of eddies takes place. Figure 1.3 shows the schematic layout of the pipe network to be used in the present study.

1.3 Problem Statement

The primary objective of the case study is to simulate turbulent flow through a sharp and smooth bend case and later calculate the minor loss factors using the

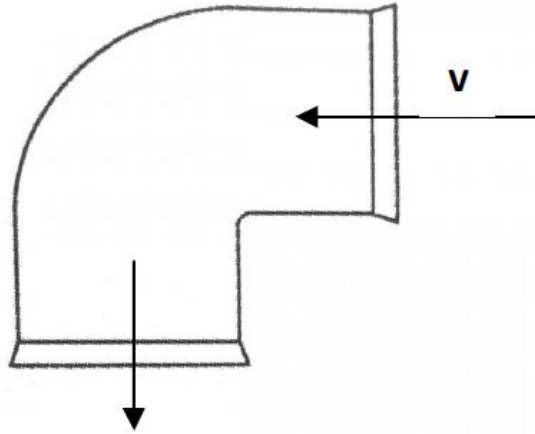


Figure 1.1: Sharp Bend[1]

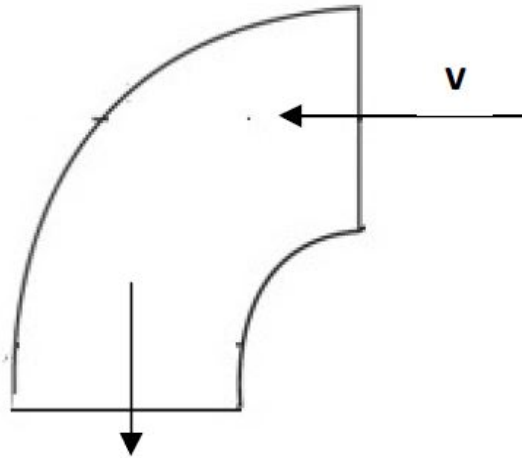


Figure 1.2: Smooth Bend[1]

CFD result and compare it with the experimental or analytical results. The dimensions of the pipe fittings are considered from the lab manual[1]. The simulations were conducted for 17 different cases. To study this turbulent flow, simpleFoam solver is used.

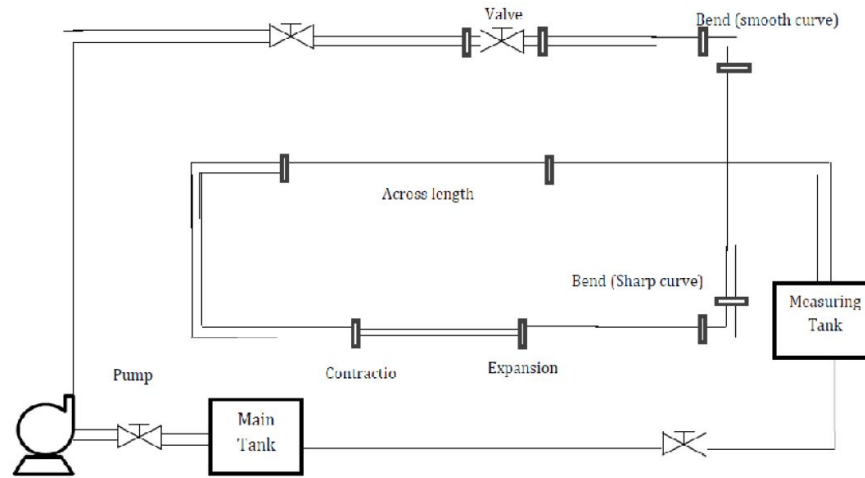


Figure 1.3: Schematic layout of pipe network with fittings[1]

1.4 Schematic Diagram

The dimensions of the geometry is given below

Diameter of the collecting tank, $D_c = 0.28$ m

Diameter of the larger cross-section pipe, $D_1 = 14.3$ mm

The geometry of smooth and sharp bend case is shown in the Figure 1.4.

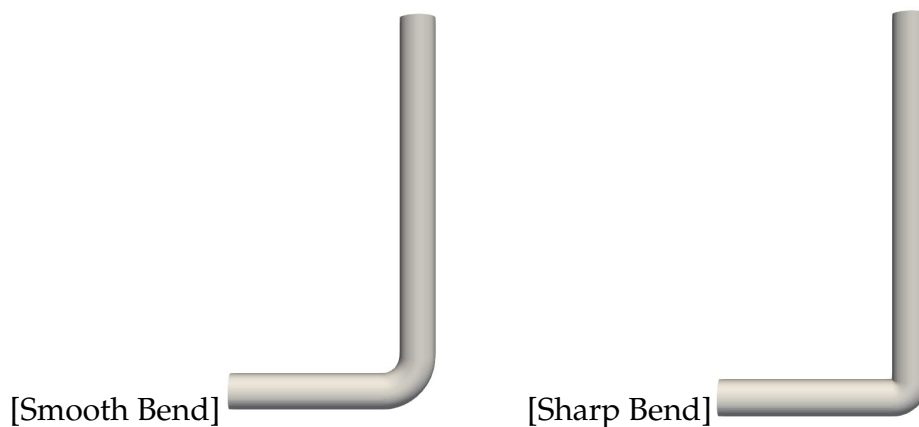


Figure 1.4: Pipe Bend

Chapter 2

OpenFOAM base case

2.1 pitzDaily

The base case considered for the simulation of the orifice meter is the pitzDaily case. This case can be found under the incompressible section, simpleFoam subsection. The directory for this is

\OpenFOAM-v1912\tutorials\incompressible\simpleFoam\pitzDaily.

Based on the experimental work of Pitz and Daily (1981). It features a backward facing step. Such a “classic” case is instructive for comparing different turbulence models with respect to the size and shape of the recirculation zone[[internet reference](#)]. pitzDaily introduces the following concepts for the first time:

- Mesh creation using blockMesh and also mesh grading capability
- Turbulent steady flow.

2.1.1 Folder Structure

Any case file in OpenFOAM has three folders, called the 0, constant and the system. The constant contains coefficient values that will be used in equations and also things which will remain constant like the mesh, material properties, environmental constants which the solver uses, the 0 folder contains the initial and boundary conditions, and the system folder contains the configuration files for the mesh and also how the solver will be executed, schemes and methods to use and controls for the simulation.



Table 2.1: Folder contents

Directories	Constant	0	System
Sub-directories	transportProperties turbulenceProperties polyMesh	U p nut omega k	blockMeshDict fvSchemes fvSolution

2.2 Solver

OpenFOAM or Open-source Field Operation And Manipulation is an open-source C++ tool used for solving continuum mechanics problems, with a focus on Finite Volume Method (FVM). The software package includes solver codes for different kinds of transport phenomena, varying from simple laplacian solver called laplacianFoam to complex multiphase flow, compressible flow, heat transfer, incompressible flow, and many more. The flagship solver and most commonly used solver is simpleFoam. simpleFoam is a steady-state solver for incompressible, turbulent flow. It utilizes the SIMPLE (Semi-Implicit Method for Pressure Linked Equations) algorithm. It is an approximation of the velocity field which is obtained by solving the momentum equation. The pressure gradient term is calculated using the pressure distribution from the previous iteration or an initial guess. The pressure equation is formulated and solved to obtain the new pressure distribution. Velocities are corrected and a new set of conservative fluxes is calculated. The solver used for this case study is simpleFoam, it employs SIMPLE algorithm. The case study considered is a steady state, incompressible, three-dimensional flow. The set of Navier Stokes equations governing the flow is given below.

The continuity equation is given as,

$$\nabla \cdot \vec{u} = 0 \quad (2.1)$$

The momentum equation is given as.

$$\frac{\partial \vec{u}}{\partial t} + \nabla \cdot [\vec{u}\vec{u}] = -\frac{1}{\rho} \nabla p + \nu \nabla^2 \vec{u} \quad (2.2)$$

Where, \vec{u} is velocity, p-pressure; ν is kinematic viscosity The discretized momentum equation and pressure correction equation are solved implicitly, where the



velocity correction is solved explicitly. This is the reason why it is called "Semi-Implicit Method".

2.2.1 Turbulence Model

The turbulence model considered for the simulation is κ - ω SST RANS model. κ - ω SST model solves two additional equations, for turbulent kinematic energy κ and specific turbulent dissipation rate ω . The equations for the κ - ω SST RANS model is given below,

$$\frac{\partial(p\kappa)}{\partial t} + \frac{\partial(p\kappa u_i)}{\partial x_i} = P - \beta^* \rho \omega \kappa + \frac{\partial}{\partial x_i} [(\mu + \sigma_\omega \mu_t) \frac{\partial \omega}{\partial x_i}] \quad (2.3)$$

$$\frac{\partial(p\omega)}{\partial t} + \frac{\partial(p\omega u_i)}{\partial x_i} = \frac{\gamma}{\nu_t} - \beta \rho \omega^2 + \frac{\partial}{\partial x_i} [(\mu + \sigma_\omega \mu_t) \frac{\partial \omega}{\partial x_i}] + 2(1 - F_1) \frac{\rho \sigma_\omega}{\omega} \frac{\partial \kappa}{\partial x_i} \frac{\partial \omega}{\partial x_i} \quad (2.4)$$

where u_i represents velocity component in corresponding direction, μ_t represents eddy viscosity. The default value of model coefficients [2] have been used.

Chapter 3

OpenFOAM Case Modifications

Using the pitzDaily case, modifications were made with the geometry, the mesh used, boundary conditions applied to it, and the control parameters which are going to be explained further in the below sections.

3.1 Pre-processing

The models for both the case was created using the dimensions from the manual provided [1]. As the geometry was complicated to be created using blockMesh utility, the geometry and the mesh was created using ANSYS Design Modeller and the mesh using the in-built software. As the geometry has 3-D mesh cells, the up-stream length was reduced and a parabolic velocity inlet boundary condition was provided to reduce the computational costs. The downstream length was about 10D.

3.2 Boundary conditions

The initial and boundary conditions are included in the 0 folder as k, omega, nut,p, and U. The boundary conditions are summarised in the Table 3.1 for both the cases. The value for κ and ω were determined using the below equations

$$\kappa = \frac{3}{2}(uI)^2 \quad (3.1)$$

$$\omega = \frac{C_{\mu}^{-0.25}\kappa^{0.5}}{0.07l} \quad (3.2)$$



Table 3.1: Boundary conditions

	inlet	outlet	wall
omega	fixedValue	zeroGradient	omegaWallFunction
k	fixedValue	zeroGradient	kqRWallFunction
nut	calculated	calculated	nutkWallFunction
p	zeroGradient	fixedValue	zeroGradient
U	codedFixedValue	zeroGradient	noSlip

where u is the free stream velocity, I is the turbulence intensity, C_μ is the model coefficient, l is the characteristic length. The inlet velocity was provided through the codedFixedVelocity, parabolic velocity was provided through this function as the upstream length was reduced.

3.3 Physical properties

The working fluid for both the simulation was water. The density considered was 1000 kg/ m^3 , with a kinematic viscosity of $1 \times 10^{-06} \text{ m}^2/ \text{s}$. The value in the transportProperties file was changed to 1×10^{-06} from 1×10^{-05} and the transportModel remained as it is to Newtonian.

3.4 fvSchemes & fvSolution

fvSchemes and fvSolutions are found under the constant folder. fvSolution directory contains equation solvers, algorithms and tolerances. No changes were done to this file, the tolerances for the residuals were pre-set to a value of $1e-05$ and it was not changed. The numerical schemes for the simulation are entered in the fvSchemes dictionary. No changes were made in this file directory.

3.5 Control parameters

The OpenFOAM solvers begin all runs by setting up a database. The database controls I/O and, since output of data is usually requested at intervals of time during the run, time is an inextricable part of the database. The controlDict dictionary



sets input parameters essential for the creation of the database. Here the `endTime` was changed to 4000, i.e., maximum iterations were 4000. `startTime` was 0 and `writeInterval` was set to every 100 iterations with 1 as `deltaT` as it was a steady state analysis.

3.6 Post-processing

After the simulation has been completed, the results were viewed in ParaView. To do this, first the results obtained were converted into viewable file using the command `touch suitable_file_name.foam`. A file with `.foam` extension was created. In this file, the results was viewed, the various contours of the solution was visualised, streamlines were plotted and the data were analysed with the in-built plotting options available.

Chapter 4

Results

Steady state simulations were performed using SIMPLE algorithm for κ - ω SST RANS model. The obtained CFD results have been compared with the experimental results for the coefficient of discharge. Post-processing was done using paraview.

4.1 Numerical Results

The post-processing of the simulation was done in ParaView for both the cases each having 17 simulations, the Reynolds number varied from 5000 to 26000. The numerical results are further discussed below.

4.1.1 Smooth Bend

The velocity and pressure contours obtained by the simulations are shown in Figure 4.1. Also, the pressure and velocity contours for higher and lower Reynolds number are also plotted in Figure 4.2 and Figure 4.3. From the contours it is seen that at the bend, there is a change in the direction of the velocity, which leads to boundary layer separation. Due to the effect of centrifugal force, the boundary layer at the inner wall is getting thicker and the boundary layer at the outer wall is getting thinner. When the centrifugal force continues to increase, the boundary layer will separate from the inner wall[3]. Due to this separation, there is a loss in head, which accounts for the minor loss.

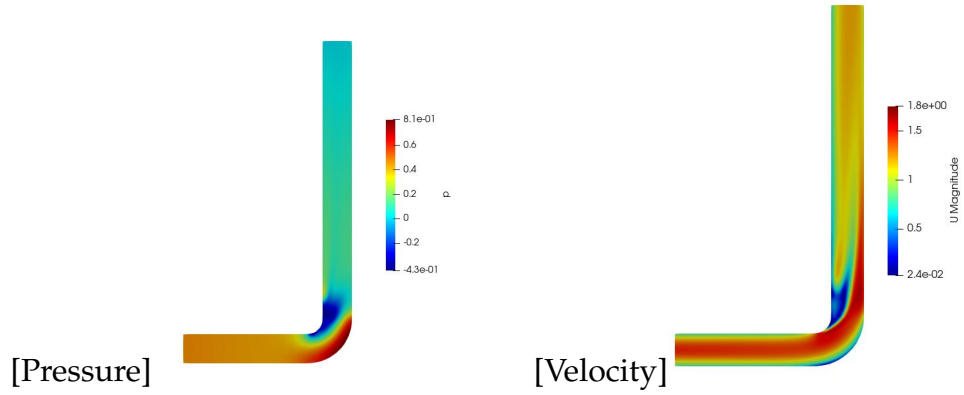


Figure 4.1: Contours

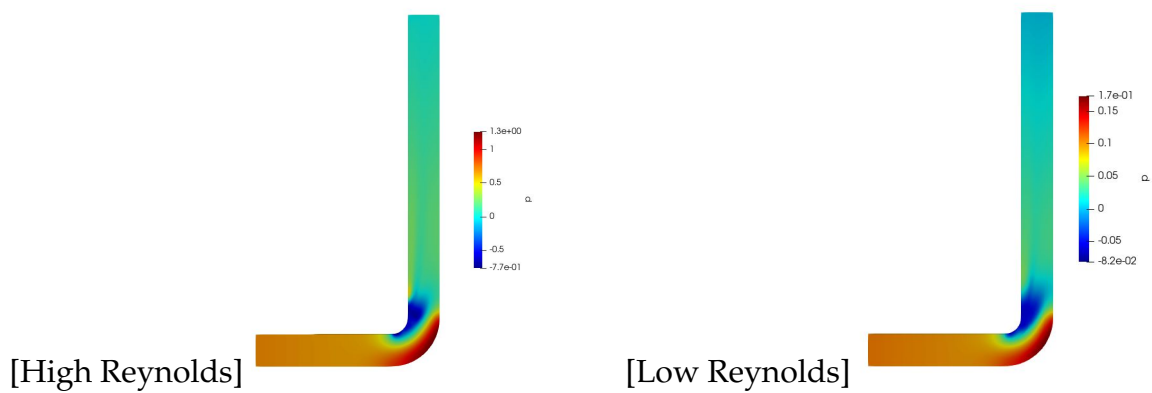


Figure 4.2: Pressure Contour

Due to the flow separation and centrifugal forces, there is a secondary flow pattern occurring at the exit of the bend. The secondary flow features include pair of counter-rotating stream-wise vortices called Dean vortices. These flow structure are further shown in the Figure 4.4. The stream-wise vortices formed are circled in red colour. Dean vortices are also plotted for higher and lower Reynolds number and are shown in Figure 4.5 and Figure 4.6 respectively. It is seen that the Dean

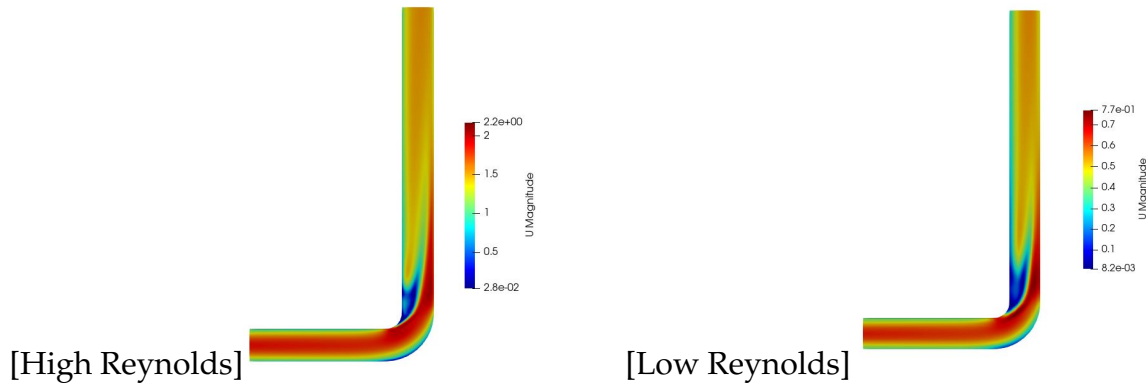


Figure 4.3: Velocity Contour

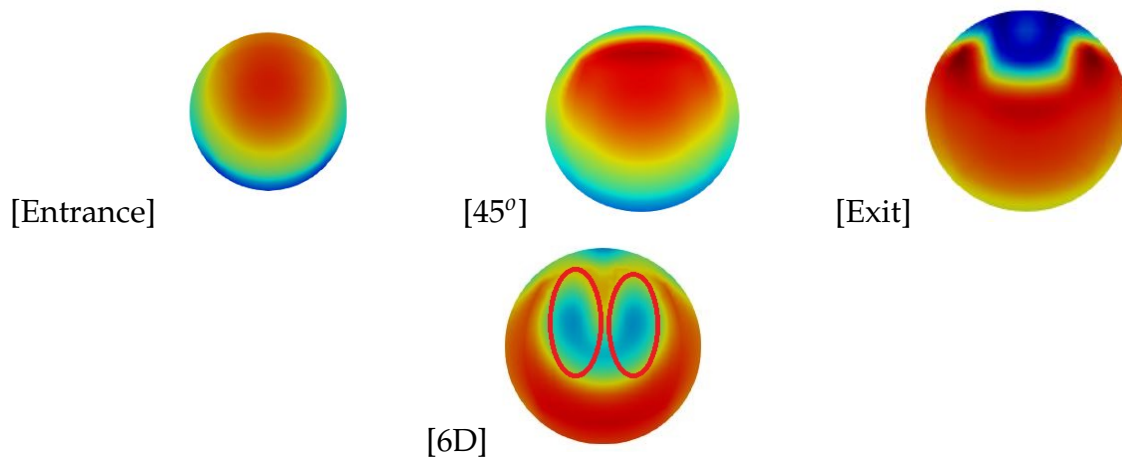


Figure 4.4: Dean vortices

vortices formed for higher Reynolds number is unsymmetrical compared to the lower Reynolds number case.

4.1.2 Sharp Bend

The velocity and pressure contours obtained by the simulations are shown in Figure 4.7. Also, the pressure and velocity contours for higher and lower Reynolds number are also plotted from Figure 4.8 and Figure 4.9. From the contours it is seen that for sharp bend, the change in the direction of the velocity is greater compared to smooth bend, which leads to larger boundary layer separation compared to smooth bend. As the separation is greater, it leads greater loss in pressure head and in turn greater minor loss compared to smooth bend.

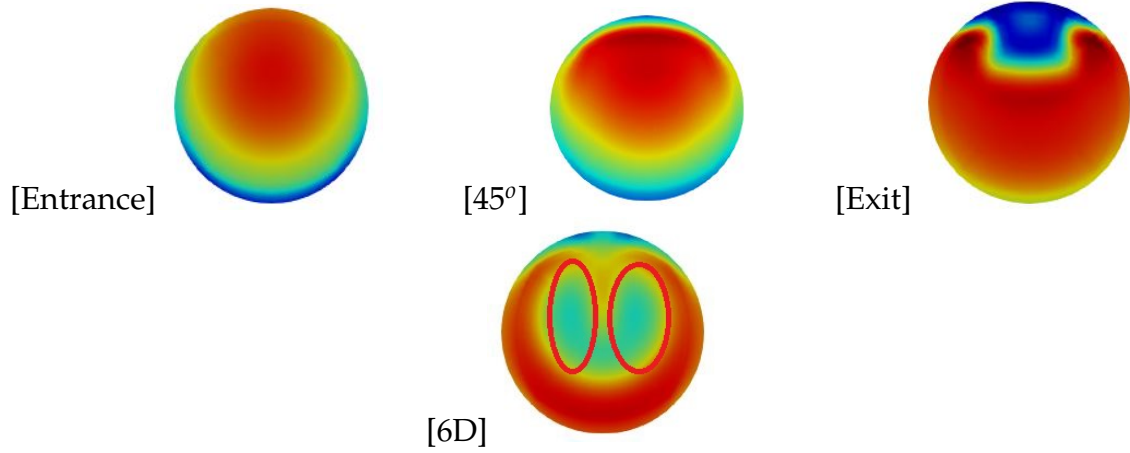


Figure 4.5: Dean vortices for Higher Reynolds number

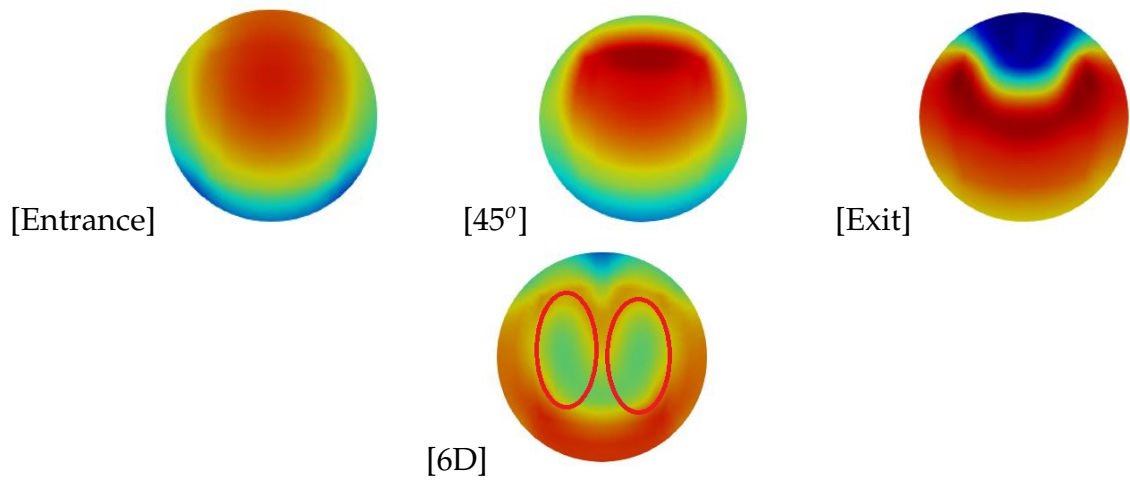


Figure 4.6: Dean vortices for Lower Reynolds number

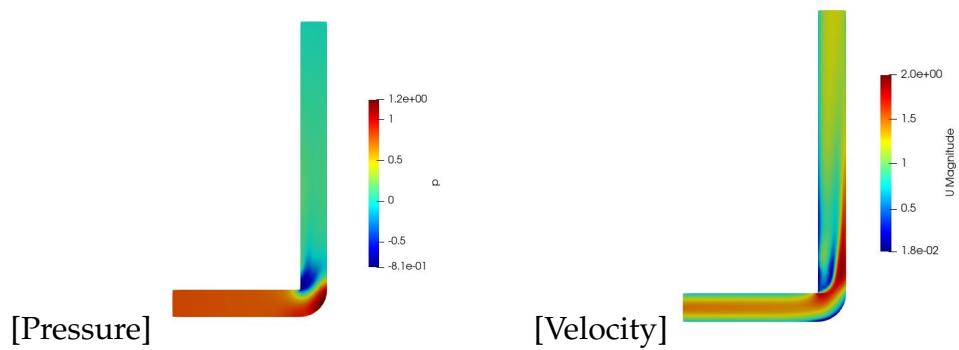


Figure 4.7: Contours

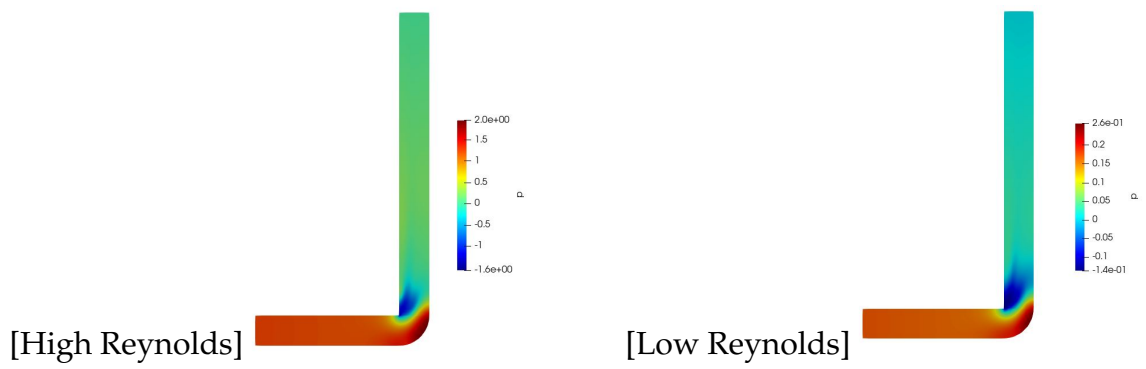


Figure 4.8: Pressure Contour

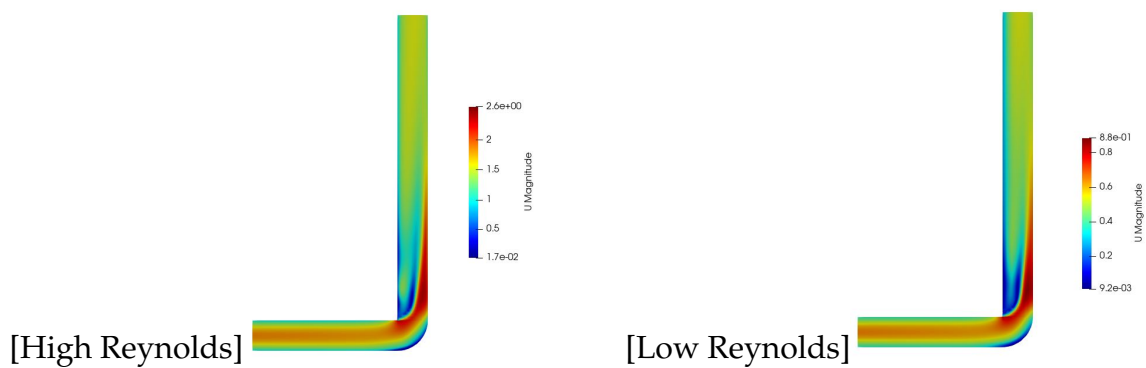


Figure 4.9: Velocity Contour

Due to the flow separation and centrifugal forces, there is a secondary flow pattern occurring at the exit of the bend. The secondary flow features include pair of counter-rotating stream-wise vortices called Dean vortices. These flow structure are further shown in the Figure 4.10. The stream-wise vortices formed here are similar to the ones that were formed in the smooth bend. These are also plotted for higher and lower Reynolds number and are shown in Figure 4.11 and Figure 4.12

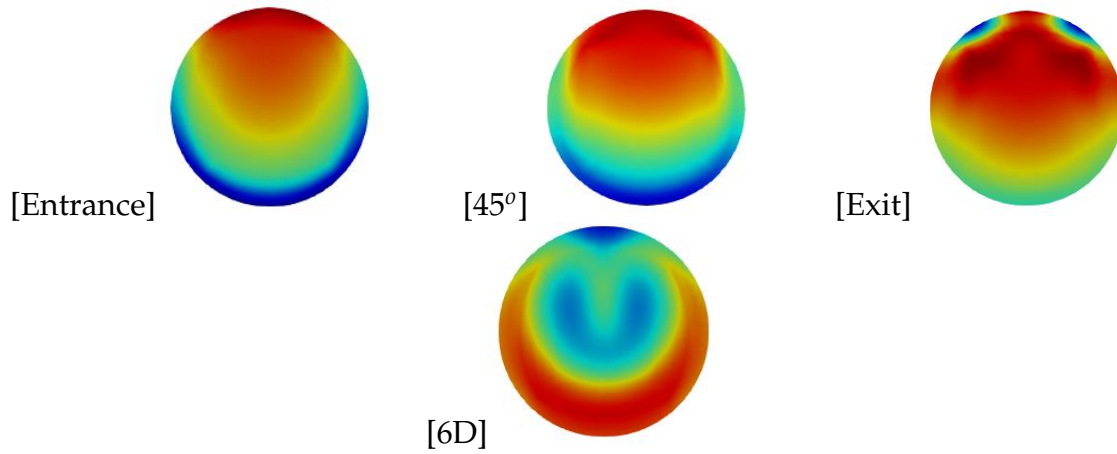


Figure 4.10: Dean vortices

respectively. Again, it is seen that the Dean vortices formed for higher Reynolds number is unsymmetrical compared to the lower Reynolds number case.

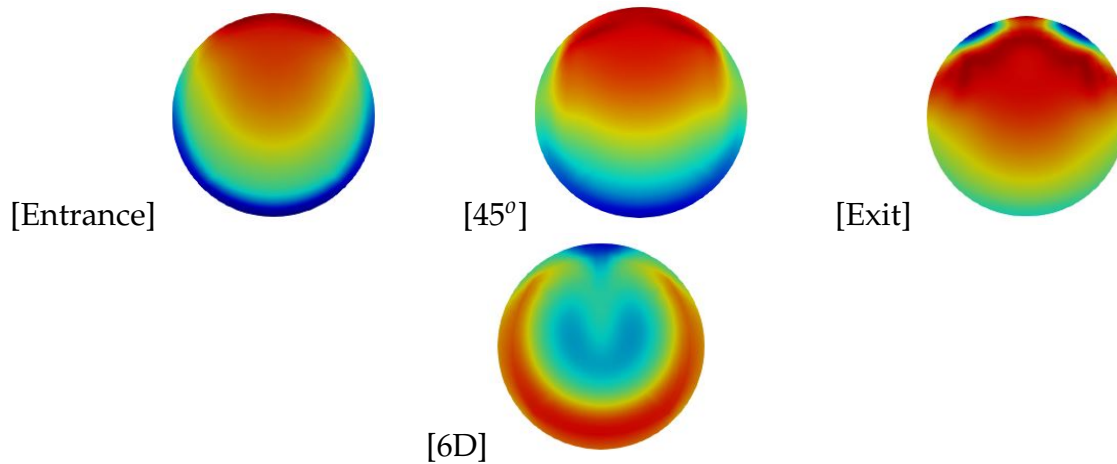


Figure 4.11: Dean vortices for Higher Reynolds number

4.1.3 Minor Loss Factors

The minor loss factors are determined for both the cases using the Equation 1.4 for both the cases. The pressure difference for the equation, was determined between the entrance of the bend and at a distance of $9D$ from the exit of the end as suggested in the paper[4]. To ensure the method was right, the minor pressure difference available in the literature was reproduced through CFD simulations and

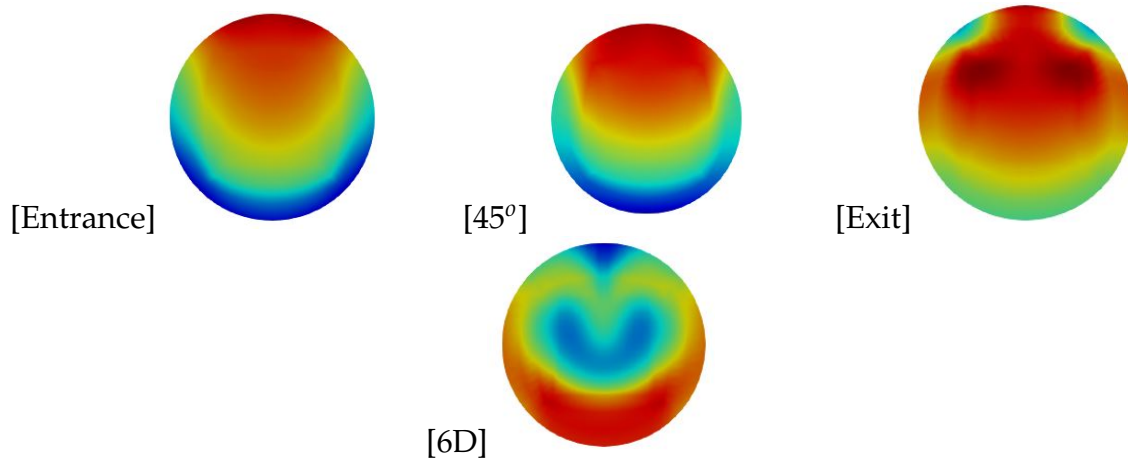


Figure 4.12: Dean vortices for Lower Reynolds number

were compared. The obtained values are summarised in Table 4.1. From Table 4.1

Table 4.1: Literature Values v/s CFD values

Velocity	Reynolds Number	k (CFD)	k (Exp)	Error
1	40000	0.224	0.26	13.84
2	80000	0.185	0.163	13.49
3	120000	0.1705	0.1429	19.31
5	200000	0.1552	0.1396	11.17

it is seen that the error between CFD and published value is less which assures the procedure through which the pressure difference obtained is right. With this, minor losses for both smooth and sharp bend is determined and is summarised in Table 4.2 and Table 4.3 respectively.



Table 4.2: CFD results for smooth bend

Sl No.	Flow rate(m^3/s)	Velocity (m/s)	Reynolds number	Turbulent kinetic energy (m^2/s^2)	Specific dissipation rate (s^{-1})	Pressure difference	K
1	0.000237	1.478038	21021	0.006858	151.0441	0.3705	0.343
2	0.000236	1.469798	20878	0.0068	150.4041	0.3625	0.3401
3	0.000202	1.25876	17875	0.00518	131.2714	0.2733	0.349
4	0.00021	1.307589	18590	0.00555	135.8788	0.29543	0.3496
5	0.000194	1.210081	17303	4.901e-3	127.6872	0.2552	0.3489
6	0.000182	1.132066	16159	4.348e-3	120.2679	0.2249	0.3524
7	0.000301	1.872526	26741	0.0105	186.8959	0.5445	0.3114
8	0.000294	1.831351	26169	0.0101	183.3014	0.5257	0.3139
9	0.000283	1.760117	25168	9.4437e-3	177.2459	0.4903	0.3165
10	0.000277	1.727316	24596	9.071e-3	173.7132	0.4693	0.3173
11	0.000288	1.792788	25597	9.727e-3	179.8849	0.5063	0.316
12	0.000291	1.812293	25883	9.918e-3	181.6424	0.5122	0.3127
13	0.000105	0.653563	9345.05	1.65e-3	74.0878	0.0849	0.402
14	0.000147	0.915238	13013	2.9772e-3	99.5197	0.1609	0.3887
15	9.88E-05	0.615353	8723	1.4785e-3	70.1319	0.085	0.4573
16	0.000106	0.659413	9295	1.6523e-3	74.1395	0.085	0.4028
17	6.29E-05	0.391737	5577	6.7586e-4	47.4169	0.03507	0.4611



Table 4.3: CFD results for sharp bend

Sl No.	Flow rate(m^3/s)	Velocity (m/s)	Reynolds number	Turbulent kinetic energy (m^2/s^2)	Specific dissipation rate (s^{-1})	Pressure difference	K
1	0.000237	1.478038	21021	0.006858	151.0441	0.607	0.5618
2	0.000236	1.469798	20878	0.0068	150.4041	0.607	0.5695
3	0.000202	1.25876	17875	0.00518	131.2714	0.4430	0.5671
4	0.00021	1.307589	18590	0.00555	135.8788	0.4783	0.566
5	0.000194	1.210081	17303	4.901e-3	127.6872	0.4158	0.5681
6	0.000182	1.132066	16159	4.348e-3	120.2679	0.364	0.5701
7	0.000301	1.872526	26741	0.0105	186.8959	0.9043	0.5172
8	0.000294	1.831351	26169	0.0101	183.3014	0.8671	0.5178
9	0.000283	1.760117	25168	9.4437e-3	177.2459	0.8031	0.5185
10	0.000277	1.727316	24596	9.071e-3	173.7132	0.7677	0.5190
11	0.000288	1.792788	25597	9.727e-3	179.8849	0.8298	0.5179
12	0.000291	1.812293	25883	9.918e-3	181.6424	0.8487	0.5181
13	0.000105	0.653563	9345.05	1.65e-3	74.0878	0.1328	0.6289
14	0.000147	0.915238	13013	2.9772e-3	99.5197	0.2545	0.6146
15	9.88E-05	0.615353	8723	1.4785e-3	70.1319	0.1176	0.6323
16	0.000106	0.659413	9295	1.6523e-3	74.1395	0.1327	0.6285
17	6.29E-05	0.391737	5577	6.7586e-4	47.4169	0.0512	0.674

Chapter 5

Conclusion

In this case study, simulation of turbulent flow through smooth and sharp bend was done using κ - ω SST RANS turbulence model. The minor loss factor was determined for both the cases in Reynolds number range of 5000-26000. Velocity, pressure contours and secondary flow features were visualised through which various distinctive flow behaviours were studied.

Bibliography

- [1] *Losses due to Pipe Fittings, Thermofluids Lab Manual, Department of Energy Science and Engineering, IIT Bombay.*
- [2] Florian R Menter. Two-equation eddy-viscosity turbulence models for engineering applications. *AIAA journal*, 32(8):1598–1605, 1994.
- [3] Yan Wang, Quanlin Dong, and Pengfei Wang. Numerical investigation on fluid flow in a 90-degree curved pipe with large curvature ratio. *Mathematical Problems in Engineering*, 2015, 2015.
- [4] Máté Bíbok, Péter Csizmadia, and Sára Till. Experimental and numerical investigation of the loss coefficient of a 90 pipe bend for power-law fluid. *PERIODICA POLYTECHNICA-CHEMICAL ENGINEERING*, 64(4):469–478, 2020.